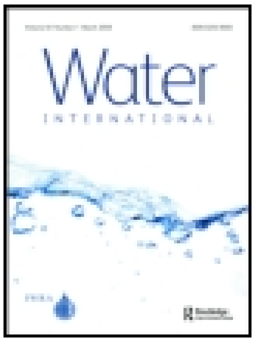

Water International

ISSN: 0250-8060 (Print) 1941-1707 (Online) Journal homepage: http://www.tandfonline.com/loi/rwin20

Analysis of the El Niño Effect on the Discharge of Selected Rivers in the Asia-Pacific Region

Daniel Cluis & Claude Laberge

International Water Resources Association
Water International, Volume 27, Number 2, Pages 279–293, June 2002

Analysis of the El Niño Effect on the Discharge of Selected Rivers in the Asia-Pacific Region

Daniel Cluis, *INRS-EAU, University of Quebec, Sainte-Foy, Canada*
and **Claude Laberge**, *STATEX, Sainte-Foy, Canada*

Abstract: *Discharge records originating from 78 rivers within the Asia-Pacific region are used to assess a possible relationship between a temporal El Niño-Southern Oscillation (ENSO) Index and regional discharges of rivers. The rivers selected have long monthly discharge series and are geographically distributed throughout the whole region. Analyses of variance are used to identify the sub-regions most teleconnected to the ENSO signal. Composite analyses show the temporal patterns of the relationships between river discharge and the ENSO signal and the possible presence of a time lagged relationship. The analyses show that the rivers of the Oceania-Pacific region are the most affected and that a majority of rivers show a similar temporal pattern, thus allowing the construction of a regional composite streamflow index. The temporal patterns of the identified relationships demonstrate the possibility of forecasting the occurrence of abnormally high or low flows (floods/droughts) months ahead of time.*

Keywords: *El Niño, composite analysis, Asia-Pacific rivers, discharge, regional patterns, temporal patterns.*

Introduction

There was a time when nuclear tests were reputed to be responsible for all climatic mishaps. Today, a South-Pacific phenomenon called El Niño, a warm water upwelling occurring in the Pacific ocean near the shores of Peru, is blamed by the media for practically any unusual weather and all local extreme meteorological events (e.g., floods, droughts, forest fires, hurricanes, tornadoes, freezing rains) occurring almost anywhere in the world. It is well known that news media, and television in particular, repeatedly present catastrophic images of disasters to the general public as the consequences of extraordinary local meteorological events.

In the context of climate variability and change, there is a lot of current research concerning the El Niño phenomenon whose frequency of occurrence appears to have increased in the last quarter century. But even with the hypothesis of stationarity (no climate change), it has always been difficult to evaluate the return period of extreme events since the length of the historically recorded hydrological series rarely exceeds one or two centuries at most, which constitutes a very short time period for assessing the tail distributions of the underlying parent population. Numerous investigations have also focused on the global nature of the atmospheric long-range circulation of air masses at the origin of meteorological events: i.e., what is the geographic extent of the influence of the ENSO phenomenon? Which regions of the world are directly or indirectly influenced by it? Such "teleconnection" may extend far beyond the South-Pacific region.

There is large body of literature devoted to the monitoring, understanding, modeling, and forecasting of the spatio-temporal evolution of ENSO in its different phases. More scarce, however, is literature related to the actual operational applications of the acquired understanding of ENSO-triggered anomalies. In most cases, relationships between the Southern Oscillation Index (SOI) and hydrometeorological episodes of interest (precipitation, discharge, floods and droughts) are established with empirical methods, researching for categorical events and significantly different parameters such as their mean values, times of occurrence, etc. Using such an approach, Shukla and Paolina (1983) have related the rain conditions for India (drought, below-average rain, above-average rain, very wet) to the phases (warm, cold) of ENSO.

Ropelewski et al. (1995) have computed the quantile distributions (10, 30, 50, 70, and 90 percentiles) of precipitation amounts occurring during different types of events (warm, neutral, and cold) of the Southern Oscillation phases for different regions of the world with demonstrated SOI-precipitation relationships. In several studies, relationships were determined between the SOI and indices, the cumulative number of events and the cumulative precipitation amounts according to whether or not they belonged to empirically defined phases of the ENSO. In fact, the state of understanding acquired by TOGA (NRC, 1996) and other programs concerning the practical consequences of ENSO is still unclear and certainly incomplete with respect to the geographical extent of ENSO-related precipitation anomalies. Thus, it is not surprising that surface water discharge anomalies directly related to abnormal rain amounts, timing, or distributions are even less well-defined. Nevertheless, some authors have succeeded in showing significant relationships between ENSO and streamflow variations in different parts of the world. For example, Simpson et al. (1993) show a significantly high proportion of low discharge in two Australian rivers (Murray and Darling) for years with warm sea surface temperature (SST) for the eastern tropical Pacific and inversely a significantly high proportion of high discharge for cold SST. Moss et al. (1994) establish that the probability of nonexceedance of 360m^3/s for the streamflow of a New Zealand river (Clutha) can be seen to increase by a factor of more than five for La Niña years in comparison to neutral years. Piechota et al. (1997), Dracup and Kahya (1994), Kahya and Dracup (1993) Piechota and Dracup (1996) study relationships between El Niño and La Niña events and river streamflow in the United States. Eltahir (1996) in North Africa (Nile river) suggests that 25 percent of the natural variability in the annual flow of the Nile is associated with El Niño oscillations. Finally, it was found that the link between ENSO, rainfall and streamflow is statistically significant in most regions of Australia (Chiew et al., 1998), but not strong enough to consistently and accurately predict rainfall and streamflow.

When relationships are found between streamflow and ENSO signals, several authors have used composite streamflow analysis in order to describe the temporal patterns of these relationships. This analysis is performed using a compounded index constructed with standardized discharge series for discriminated categorical years (Niño, Niña, and normal). Guetter and Georgakakos (1996) performed such an analysis on the Iowa River in the United States, Piechota et al. (1997) on groups of several rivers in the western United States, and Kim and Lee (2000) on two Korean rivers.

In this paper, we take advantage of the availability of a very large database of historical long-term discharge series for numerous rivers in the world at the Global Runoff Data Centre (GRDC), to relate these discharge (and especially their high and low values) to the different phases of ENSO; i.e., to test the significance of the differences in discharge distributions for normal and El Niño years. Although data are available for rivers in all continents, the present study considers only Asian and Oceanian rivers. It is believed that the relative magnitude of discharge is a good integrated index for a possible teleconnection as it results from the magnitude and time of occurrence of precipitation over the whole basin, despite its convoluted transportation within the terrestrial part of the hydrologic cycle.

This study will investigate whether the different years can be statistically differentiated on the basis of their discharge responses to a SOI index. El Niño is currently monitored in almost real time and forecasts are made regularly on its development; thus, if the regions under El Niño influence were known, as well as the temporal pattern of the discharges (relative magnitude and timing of occurrence for "normal" and El Niño years), this would be of definite practical interest for agriculture (selection of the next crop, for example) and operational hydrology (management of dam and reservoir levels).

Data Description

Discharge Data

The discharge data were directly selected from the GRDC data bank using the GRDC Catalogue Tool software (Version 2.1 for Windows 95-NT). This software allows the user to query for data according to specific successive selection criteria, such as daily or monthly data series, according to WMO region (six continental entities), sub-region (regional entities or watersheds), river name, GRDC station number, country code, range of operational years, or size of river basin.

Once the query file for stations is completed, the GRDC database system extracts the required selected data and provides them to the user as an ASCII file. In this case, stations with monthly records from WMO Regions 5 (Oceania-Pacific) and 2 (Asia) were extracted from the GRDC database. A working data set of 78 stations was obtained by using the following criteria as selection guidelines:

- Length of operation: The selected stations present a record of a minimum of 25 recent years of continuous operation, with generally less than 5 percent missing data (only eight stations with more than 5 percent but less than 10 percent missing data were selected).
- Regional representativity: The selected stations should drain large areas, making them representative of their climatic regions and less sensitive to local meteorological events.
- Geographic distribution: The chosen stations are distributed throughout the whole Asia-Pacific region according to the availability of long-term series within the database and to their adherence to the selection criteria. They are grouped into five regional geographic subsets to allow possible regionalization of the obtained results. These five subsets are: Oceania-Pacific (19 rivers), South-East Asia (9 rivers), Far East Asia (25 rivers), the Indian Subcontinent (11 rivers), and Central Asia (13 rivers). The locations of the gauging stations are shown in Figure 1.

According to GRDC procedures, countries provide their discharge data for storage in the database and are solely responsible for the quality of these data. The selected stations of the Asia-Pacific region used for this study are presented in Table 1. The table presents, for each river, its GRDC station number, an identification code for location on Figure 1, the country location code, the name of the river and the related gauging station, its longitude and

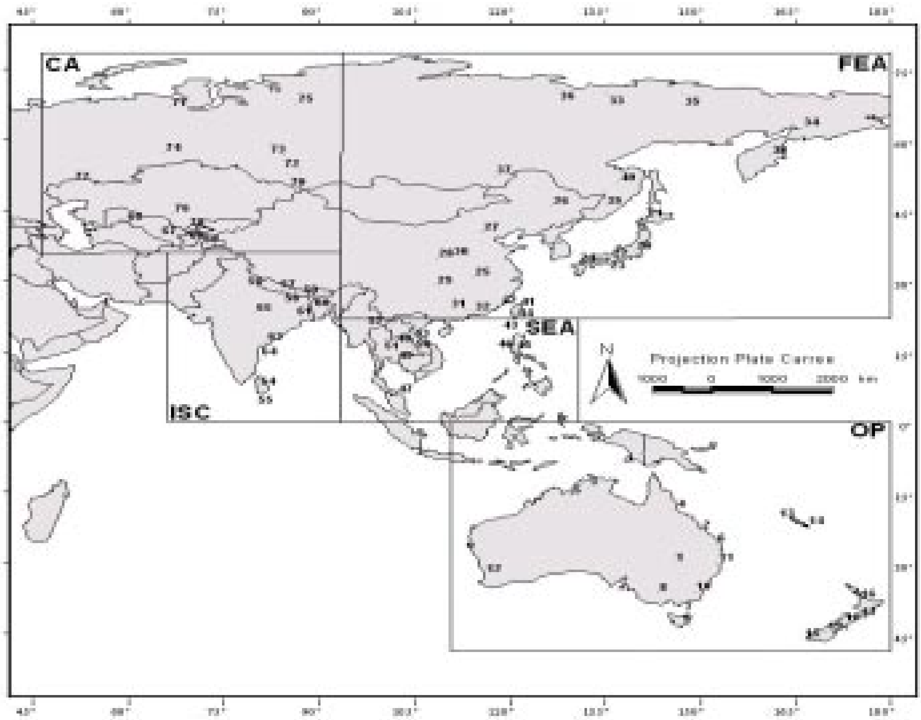

Figure 1. Locations of rivers studied in Asia and Oceania. The number representing each river is shown in Table 1. CA = Central Asia, FEA = Far East Asia, ISC = Indian Subcontinent, SEA = South East Asia, and OP = Oceania Pacific.

latitude, the watershed area, the first and last full year of operation, the percentage of missing data and the total length of the record in years. The data extracted from the database and used throughout the analysis are the monthly discharges from which yearly values were compounded.

The Southern Oscillation Index (SOI) Data

The El Niño Southern Oscillation (ENSO) is a phenomenon, which affects the large-scale meteorological behaviour of the tropical Pacific Ocean. This oscillation can be characterized by indices based either on variations of sea temperatures (Sea Surface Temperature anomalies [SST] such as the Kaplan values available for the Niño3 area) or on differences in barometric pressure measured at sea level. In this report, the Southern Oscillation Index (SOI) will be used to quantify the strength of the Walker circulation across the Pacific at the origin of the phenomenon. This index is published and updated regularly by the Australian Bureau of Meteorology and is computed, using a method developed by Troup (1965), as the standardized anomaly of monthly Mean Sea Level Pressure (MSLP) differences, measured at Papeete, Tahiti (149.6° W, 17.5° S) and Darwin, Australia (139.9° E, 12.4° S). It is calculated as follows:

$$SOI = 10 * [P_{diff} - P_{diffave}] / SD(P_{diff})$$

where: P_{diff} = Tahiti MSLP - Darwin MSLP; $P_{diffave}$ = long term average (1951-1981) of P_{diff} for the month; and $SD(P_{diff})$= standard deviation of P_{diff} for the month.

Other indices have been proposed by the Climate Prediction Center of NOAA-NCEP, Washington, DC, USA (Ropelewski and Jones, 1987), by the Climate Diagnostics Center of NOAA-CIRES, Boulder, Colorado, USA (Wolter and Timlin, 1998), and others. The differences between them are limited to the number of variables taken into account, the period of reference, and whether or not distributions were normalized.

With the SOI definition discussed earlier, negative values of the index (< -5) correspond to the "warm" phase (low SOI) of the ENSO index, often referred to as the El Niño event; positive values (> +5) correspond to the "cold" phase (high SOI) of the ENSO index, also called La Niña event. El Niño and La Niña years are identified by smoothing the monthly SOI values by an 11-point moving average and selecting years with five consecutive months or more with smoothed SOI values lower than -5 or higher than +5 respectively, and lasting at least three seasons. El Niño and La Niña months are identified by smoothing the monthly SOI values by a five-point moving average and selecting strings of five consecutive months or more, with smoothed SOI values lower than -5 or higher than +5 respectively, and lasting at least three seasons.

In the literature, details regarding the precise definitions of either the year or seasons are not given, both characteristics being related to the particular climate and regime of the region under study. Given this situation, Table 2 presents the labelling of years used for this study according

Table 1. Characteristics of the Selected Rivers by Area

# on Fig. 1	River	Station	Country Code	Latitude	Longitude	Watershed Area	Begin Year	End Year	Percent Missing Data	Duration (Years)
				Ocean-Pacific Area						
1	Darling	Bourke Town	AU	3009S	14594E	386000	1944	1993	2.9	49
2	Fitzroy	The Gap	AU	2310S	15010E	135860	1965	1995	2.5	30
3	Daly	Mount Nacar	AU	1383S	13241E	47000	1970	1995	3.4	25
4	Herbert	Ingham	AU	1863S	14613E	8805	1916	1996	1.4	80
5	Mary (1)	Mount Bundy	AU	1292S	13165E	5700	1957	1995	0.6	38
6	Mary (2)	Miva	AU	2595S	15250E	4830	1910	1995	0	85
7	Mitchell	Glenaladale	AU	3775S	14737E	3900	1938	1987	2.4	49
8	Avoca	Coonooer	AU	3644S	14330E	2670	1890	1993	1.3	103
9	Huon	Frying Pan Creek	AU	4304S	14684E	2097	1949	1994	0.9	45
10	Murrumbridgee	Mittagang Cross.	AU	3618S	14909E	1891	1927	1993	1.1	66
11	Nymboida	Nymboida	AU	2998S	15272E	1660	1909	1993	2.6	84
12	Serpentine	Serpent. Falls	AU	3237S	11601E	769	1911	1992	0.9	81
13	Tipindje	Ouen-Kout	NC	2078S	16499E	247	1956	1984	1.4	28
14	Riviere Des Lacs	Goulet	NC	2223S	16685E	69	1958	1984	0	26
15	Mataura	Gore Hbr	NZ	4610S	16895E	3465	1961	1993	0	32
16	Motu	Houpoto	NZ	3786S	17765E	1393	1958	1990	1.7	32
17	Ongarue	Taringamutu	NZ	3886S	17524E	1075	1963	1994	0	31
18	Hurunui	Mandamus	NZ	4279S	17255E	1070	1957	1990	4.2	33
19	Ahuriri	Sth Diadem	NZ	4447S	16973E	557	1964	1994	0	30
				Far East Area						
20	Tone	Kurihashi	JP	3613N	13970E	8588	1938	1986	6.1	48
21	Ishikari	Ishikari-Ohashi	JP	4312N	14153E	12697	1954	1986	6.3	32
22	Shinan	Ojiya	JP	3730N	13880E	9719	1965	1988	4.5	23
23	Yodo	Hirakata	JP	3480N	13563E	7281	1965	1988	4.2	23
24	Chikugo	Senoshita	JP	3353N	13080E	2315	1965	1988	4.2	23
25	Changjiang	Hankou	CI	3058N	11428E	1488036	1865	1986	1.2	121
26	Songhuajiang	Haerbin	CI	4577N	12658E	391000	1898	1987	4.4	89
27	Yongding	Guanting	CI	4023N	11560E	42500	1925	1988	6.6	63
28	Jinghe	Zhangjiashan	CI	3463N	10860E	43200	1933	1986	7.6	53
29	Wujiang	Gongtan	CI	2890N	10835E	58300	1939	1982	9.1	43
30	Huanghe	Huayuankou	CI	3492N	11365E	730036	1947	1988	5.2	41
31	Beijiang	Hengshi	CI	2385N	11327E	34013	1954	1987	1	33
32	Dongliang	Boluo	CI	2317N	11430E	25325	1960	1987	0	27
33	Yana	Dzanghky	RS	6967N	13533E	216000	1938	1984	1.8	46
34	Penzhina	Kamenskoe	RS	6242N	16603E	71600	1957	1984	3.6	27
35	Indigirka	Vorontsovo	RS	6958N	14735E	305000	1937	1994	1	57
36	Lena	Kusur	RS	7070N	12765E	2430000	1935	1994	0	59
37	Shika	Sretensk	RS	5225N	11772E	175000	1897	1985	1.9	88
38	Kamchatka	Kluchi	RS	5643N	16105E	45600	1931	1984	0.8	53
39	Amur (1)	Khabarovsk	RS	4843N	13505E	1630000	1897	1985	0.9	88
40	Amur (2)	Komsomoisk	RS	5063N	13712E	1730000	1933	1990	0	57
41	Li-Wu	Lu-Shui	TW	2418N	12150E	435	1960	1993	0	33
42	Yugeng	Dahan	TW	2465N	12128E	335	1964	1989	0	25
43	Sandimen	Ailiao	TW	2270N	12063E	408	1964	1989	0	25
44	Xinfadaqiao	Laonong	TW	2305N	12065E	812	1964	1989	0	25
				South East Asia Area						
45	Pampanga	San Agustin	PH	1517N	12078E	6487	1946	1974	5.7	28
46	Bonga	Bangay	PH	1808N	12070E	534	1947	1976	6.1	29
47	Kelantan	Guillemard Bridge	MS	577N	10215E	11900	1950	1986	7.7	37
48	Mekong (1)	Mukdahan	TH	1653N	10473E	391000	1925	1991	0.4	66
49	Nam Chi	Yasothon	TH	1578N	10415E	43100	1954	1991	0.6	37
50	Nam Mun	Ubon	TH	1522N	10487E	104000	1956	1991	1.1	35
51	Nan	Sirkit Dam	TH	1777N	10055E	13300	1956	1988	2.9	32
52	Mekong (2)	Chiang Saen	TH	2027N	10010E	189000	1961	1991	1	30
53	Mekong (3)	Nakhon Phanom	TH	1740N	10480E	373000	1962	1991	3.3	29

Table 1. Characteristics of the Selected Rivers by Area (Continued)

# on Fig. 1	*River*	*Station*	*Country Code*	*Latitude*	*Longitude*	*Watershed Area*	*Begin Year*	*End Year*	*Percent Missing Data*	*Duration (Years)*
					Indian Subcontinent Area					
54	Mahaweli Ganga	Peradeniya	SB	727N	8058E	1189	1950	1984	2.8	34
55	Gin Ganga	Agaliya	SB	618N	8020E	681	1928	1989	1.7	61
56	Karnali River	Chisapani	NE	2864N	8129E	42890	1962	1993	0	31
57	Kali Gandaki (1)	Setibeni	NE	2801N	8360E	6630	1964	1993	0.3	29
58	Kali Gandaki (2)	Kotagaon Shringe	NE	2755N	8435E	11400	1964	1985	4.2	21
59	Tamur River	Mulghat	NE	2693N	8733E	5640	1965	1986	0	21
60	Ganges R. (1)	Harlinge Bridge	BW	2408N	8903E	846300	1934	1989	2.1	55
61	Ganges R. (2)	Farakka	IN	2500N	8792E	935000	1949	1985	0	36
62	Sapt Kosi	Barashetra	NE	-	-	-	1947	1978	0	31
63	Godavari	Polavaram	IN	1692N	8178E	299320	1902	1979	7	77
64	Krishna	Vijayawada	IN	1652N	8062E	251355	1901	1979	6.3	78
65	Narmada	Jamtara	IN	2302N	7933E	16576	1949	1974	0.3	25
					Central Asia Area					
66	Amu-Darya	Chatly	UZ	4228N	5970E	450000	1931	1973	2..1	42
67	Zaravchan	dupuli	TA	3938N	6777E	10200	1932	1994	1.3	62
68	Gunt	Khorog	TA	3753N	7152E	13700	1940	1985	0	45
69	Vakhsh	Tutkaul	TA	3833N	6930E	31200	1932	1967	1.6	35
70	Biya	Biysk	RS	5252N	8527E	36900	1895	1985	0	90
71	Ob	Salekhard	RS	6657N	6653E	2949998	1930	1994	0	64
72	Tom (1)	Novokuznetsk	RS	5375N	8710E	29800	1894	1985	0	91
73	Tom (2)	Tomsk	RS	5658N	8487E	57000	1965	1990	0	25
74	Tura	Tiumen	RS	5715N	6553E	58500	1896	1985	0	89
75	Yenisel	Igarka	RS	6748N	8650E	2440000	1936	1995	0	59
76	Sri-Darya	Tyumen-Aryk	KZ	4405n	6705e	219000	1930	1984	7	54
77	Ural	Kushum	KZ	5085N	5128E	190000	1915	1984	4.3	69
78	Naryn	Uch-Kurgan	KG	4117N	7210E	58400	1933	1990	0	57

to previously defined criteria, with the restriction that it uses calendar years and disregards the number of seasons that should be present to constitute an event. Periods that were not labelled as belonging to either El Niño or La Niña events were considered as normal or neutral conditions and were used as a reference.

It should also be noted that some researchers, recognizing the fact that some El Niño events lasted more than one year, have tried to differentiate the months of the first year or rising limb by using a subscript 0, whereas the months of the second year or sinking limb were subscripted +1; in this study, however, no such differentiation was attempted.

Statistical Approach

In this study, the classical ANOVA procedure and the Kruskall Wallis test were used to test the hypotheses (Conover, 1980; Montgomery, 1984):

H_0 : $\mu_{nina} = \mu_{normal} = \mu_{nino}$ (No teleconnection between ENSO and river discharge)

vs H_1: At least two of the means are different (Teleconnection between ENSO and river discharge).

Where μ_{nina}, $\mu_{normal,}$ and μ_{nino} are the discharge means for the years of La Niña, Normal, and El Niño phases, respectively, which are three exclusive modalities of the ENSO factor. The main distinction between these tests is the fact that ANOVA tests are parametric tests performed directly on measured values, whereas Kruskall-Wallis tests are non-parametric tests performed on the ranks associated with the measured values. The ANOVAS are performed using the SAS System GLM procedure, whereas the Kruskall-Wallis tests were performed using the SAS System procedure RANKS followed by the GLM procedure on the ranks. Duncan's multiple comparison test was used to determine which means are significantly different from one another when H_0 is rejected. The results of Duncan's tests are summarized by letters in parentheses following numerical mean values. Two means with the same letter are not significantly different. Note that a code (AB) means A or B, so a level with this code is neither significantly different from a level with the code (A) nor from a level with the code (B). Duncan's test is used as an option in the SAS GLM procedure.

Table 2. Classification of Years According to an Identification as El Niño, La Niña, or Normal Years

Period 1876–1900			*Period 1901–1925*			*Period 1926–1950*			*Period 1951–1975*			*Period 1976–1997*		
Niño	*Normal*	*Niña*	*Niño*	*Normal*	*Niña*	*Niño*	*Normal*	*Niña*	*Niño*	*Normal*	*Niña*	*Niño*	*Normal*	*Niña*
	1876			1901		1926				1951			1976	
1877				1902			1927			1952		1977		
		1878			1903			1928	1953				1978	
		1879			1904		1929			1954			1979	
		1880	1905				1930				1955		1980	
	1881				1906		1931				1956		1981	
	1882			1907			1932		1957			1982		
	1883			1908			1933		1958			1983		
	1884				1909		1934			1959			1984	
1885					1910		1935			1960			1985	
		1886	1911				1936			1961			1986	
	1887		1912				1937				1962	1987		
1888			1913					1938		1963				1988
		1889	1914					1939			1964			1989
		1890		1915		1940			1965				1990	
	1892			1917			1942		1967		1992			
		1893		1918				1943		1968		1993		
	1894		1919				1944			1969		1994		
	1895			1920			1945				1970		1995	
1896					1921	1946					1971			1996
1897				1922			1947		1972			1997		
	1898			1923			1948				1973			
	1899				1924		1949				1974			
	1900		1925					1950			1975			

Note that Duncan's test is parametric and is therefore affected by outliers and non-normal distributions. When the Kruskall-Wallis test and the ANOVA do not draw the same conclusion, Duncan's test should be considered with the same reservations as the ANOVA results. It must also be noted that when the ANOVA results are not significant ($p > 0.05$), Duncan's test results should not be considered reliable. Duncan's test is liberal and may detect differences even if the ANOVA concluded that no significant difference exists. In this case the ANOVA test is more reliable in order for ensuring a global significance level of 5 percent. In this paper, a river is defined as being affected by the El Niño (or La Niña) phase when μ_{NINO} is significantly different from μ_{NORMAL} (or μ_{NINA} is significantly different from μ_{NORMAL}).

The composite analysis is used to describe the relationships between El Niño and La Niña years with the occurrence of high or low flows in the studied rivers. The composite analysis consists of the following steps:

- River streamflows (q_{mn}) are first transformed as: $x_{mn} = \ln(q_{mn})$;
- The transformed x_{mn} are then standardized using $z_{mn} = (x_{mn} - \mu_m)/s_m$ for each month m and each year n, the mean and standard deviation being obtained for each month. The z_{mn} are called streamflow indices;
- Composite streamflow indices are obtained for El Niño (or La Niña, or Normal) from the streamflow indices by averaging, for a given month, the streamflow indices of all El Niño (or La Niña, or Normal) years. The El Niño composite streamflow index is calculated for 36 consecutive months; Year 0 corresponds to the year preceding an El Niño year, Year 1 corresponds to an El Niño year and Year 2 corresponds to the year following an El Niño year. The same averaging is performed for La Niña or Normal years. All years are considered independently, so for consecutive El Niño (or La Niña, or Normal) years, the year preceding an El Niño year may also be an El Niño year. Note that if a dataset contains ten El Niño years, then the El Niño composite streamflow index for each of the 36 months is obtained by averaging ten streamflow indices.

When performed on a group of rivers to obtain a regional composite analysis, the streamflow indices (after transformation and standardization) are averaged for all rivers in the region, giving each river the same unit weight in the regional composite streamflow index.

Results And Discussion

Analyses of Variance

The results presented here constitute a fraction of the actual work done with the GRDC databank. The reader interested in more detailed results should refer to Cluis (1998). In Tables 3 through 7 the general results of the

Table 3. Duncan Test, ANOVA, and Kruskall-Wallis (K.W.)Results for the Discrimination of El Niño, La Niña, and Neutral Years in the Oceania Pacific Area

River	*La Niña*	*Neutral*	*El Niño*	*ANOVA*	*K.W.*
	Mean	Mean	Mean	P-value	P-value
		Mean Yearly Flows (m^3/s)			
Darling River	2222(A)	861(B)	538(B)	**<u>0.0048</u>**	**<u>0.0017</u>**
Fitzroy	254.2(A)	129.0(A)	152.4(A)	0.30	0.0529
Daly	212.9(A)	215.7(A)	204.1(A)	0.99	0.81
Herbert River	118.3(A)	103.0(A)	98.6(A)	0.59	0.51
Mary River (1)	47.4(A)	53.5(A)	44.5(A)	0.72	0.61
Mary River (2)	54.5(A)	33.3(B)	30.9(B)	**<u>0.0254</u>**	0.15
Mitchell River	38.5(A)	27.4(B)	19.2(B)	**<u>0.0031</u>**	**<u>0.0016</u>**
Avoca River	92.9(A)	16.2(B)	51.3(AB)	**<u>0.0479</u>**	**<u>0.0002</u>**
Huon River	85.7(A)	82.6(A)	84.7(A)	0.89	0.70
Murrumbidgee River	1078.8(A)	801.7(AB)	579.2(B)	0.09	0.14
Nymboida River	2730.2(A)	2148.7(AB)	1549.1(B)	**<u>0.0066</u>**	**<u>0.0210</u>**
Serpentine River	5.42(A)	4.81(A)	3.52(A)	0.33	0.36
Tipindje	10.51(A)	9.76(A)	8.27(A)	0.81	0.72
Riviere Des Lacs	4.37(A)	5.54(A)	4.12(A)	0.13	0.10
Mataura	54.4(B)	63.4(AB)	76.9(A)	**<u>0.0169</u>**	**<u>0.0211</u>**
Motu	105.1(A)	85.1(B)	83.9(B)	**<u>0.0249</u>**	0.06
Ongarue	35.6(A)	31.9(A)	32.9(A)	0.42	0.54
Hurunui	51.3(A)	49.4(A)	52.6(A)	0.78	0.78
Ahuriri	21.6(A)	24.5(A)	23.5(A)	0.37	0.35
		Monthly Maximum (m^3/s)			
Darling River	8015(A)	3785(AB)	2148(B)	**<u>0.0431</u>**	**<u>0.0116</u>**
Fitzroy	1771.3(A)	796.5(A)	1218.1(A)	0.34	0.08
Daly	1259.4(A)	1405.8(A)	1344.9(A)	0.97	0.68
Herbert River	551.6(A)	541.8(A)	506.5(A)	0.91	0.69
Mary River (1)	322.6(A)	370.7(A)	336.3(A)	0.88	0.86
Mary River (2)	327.6(A)	181.7(B)	169.9(B)	**<u>0.0314</u>**	0.49
Mitchell River	97.7(A)	88.3(AB)	58.1(B)	**<u>0.0488</u>**	**<u>0.0381</u>**
Avoca River	396.0(A)	88.5(A)	287.2(A)	0.11	**<u>0.0024</u>**
Huon River	214.3(A)	185.4(A)	184.6(A)	0.36	0.25
Murrumbidgee River	3291.3(A)	2608.3(AB)	1798.3(B)	0.12	0.077
Nymboida River	9969(A)	7535(AB)	5424(B)	**<u>0.0074</u>**	**<u>0.0229</u>**
Serpentine River	22.0(A)	18.7(A)	15.6(A)	0.53	0.49
Tipindje	40.3(A)	43.1(A)	46.8(A)	0.92	0.86
Riviere Des Lacs	13.1(A)	17.4(A)	13.0(A)	0.13	0.18
Mataura	110.0(B)	121.4(AB)	157.3(A)	0.06	0.08
Motu	214.0(A)	177.6(A)	187.3(A)	0.15	0.14
Ongarue	85.9(A)	64.8(B)	75.7(AB)	0.07	**<u>0.0281</u>**
Hurunui	109.8(A)	98.8(A)	109.8(A)	0.65	0.39
Ahuriri	45.7(A)	47.0(A)	47.6(A)	0.95	0.95
		Monthly Minimum (m^3/s)			
Darling River	185(A)	79(B)	26(B)	**<u>0.0006</u>**	**<u>0.000</u>**
Fitzroy	21.6(A)	1.98(A)	1.35(A)	0.82	0.07
Daly	16.2(A)	18.3(A)	15.8(A)	0.66	0.21
Herbert River	8.11(A)	5.13(B)	3.12(B)	**<u>0.0023</u>**	**<u>0.002</u>**
Mary River (1)	0.04(A)	0.01(B)	0.00(B)	0.30	0.18
Mary River (2)	3.24(A)	1.89(B)	1.12(B)	**<u>0.0046</u>**	**<u>0.014</u>**
Mitchell River	3.00(A)	2.04(A)	1.77(A)	0.21	0.72
Avoca River	0.59(A)	0.43(A)	0.77(A)	0.79	0.41
Huon River	14.6(A)	19.7(A)	19.5(A)	0.25	0.19
Murrumbidgee River	91.5(A)	87.2(A)	72.9(A)	0.69	0.69
Nymboida River	497.5(A)	431.9(A)	305.3(B)	0.08	0.07
Serpentine River	00.0(A)	0.05(A)	0.09(A)	0.39	0.39
Tipindje	0.75(A)	0.46(AB)	0.00(B)	0.12	**<u>0.038</u>**
Riviere Des Lacs	0.00(A)	0.31(A)	0.29(A)	0.22	0.36
Mataura	19.5(B)	27.5(AB)	33.4(A)	**<u>0.0256</u>**	**<u>0.032</u>**
Motu	30.4(A)	25.8(AB)	18.1(A)	0.06	0.16
Ongarue	8.6(A)	11.4(A)	12.3(A)	0.13	0.15
Hurunui	20.7(A)	23.9(A)	25.1(A)	0.40	0.64
Ahuriri	45.7(A)	47.0(A)	47.6(A)	0.95	0.95

Numbers with a common letter between parenthesis are not discrimated by the Duncan test on the equality of several mean values. Bold and underline indicate a significant result at the 5 percent significance level.

Table 4. Duncan Test, ANOVA, and Kruskall-Wallis (K.W.) Results for the Discrimination of El Niño, La Niña, and Neutral Years in the Far East Area

River	*La Niña*	*Neutral*	*El Niño*	*ANOVA*	*K.W.*
	Mean	*Mean*	*Mean*	*P-value*	*P-value*
			Mean Yearly Flows (m³/s)		
Tone	247.7(A)	246.5(A)	266.9(A)	0.70	0.49
Ishikari	529.8(A)	423.2(B)	479.3(AB)	**0.0263**	**0.0103**
Shinano	496.6(A)	507.5(A)	592.9(A)	0.41	0.96
Yodo	270.6(A)	248.3(A)	309.1(A)	0.44	0.61
Chikugo	101.6(A)	109.7(A)	148.8(A)	0.11	0.08
Changjiang	23556(A)	23369(A)	22808(A)	0.66	0.52
Songhuajiang	1161.7(A)	1228.0(A)	1204.0(A)	0.85	0.95
Yongding	42.3(A)	35.8(A)	36.0(A)	0.51	0.67
Jinghe	60.7(A)	60.0(A)	64.0(A)	0.88	0.89
Wujiang	1127.2(A)	1185.9(A)	1081.5(A)	0.41	0.47
Huanghe (Yellow River)	1458.9(A)	1468.5(A)	1312.7(A)	0.65	0.60
Beijiang	1224.3(A)	1023.0(A)	1039.0(A)	0.24	0.33
Dongjiang	7907.(A)	718.6(A)	790.9(A)	0.61	0.85
Yana	843.6(B)				
Pnezhina	662.2(A)	710.6(A)	700.0(A)	0.82	0.83
Indigirka	1518.7(A)	1701.8(A)	1483.4(B)	0.06	0.11
Lena	16854(A)	16664(A)	16325(A)	0.75	0.78
Shilka	403.7(A)	415.9(A)	396.7(A)	0.89	0.79
Kamchatka	779.5(A)	775.5(A)	786.4(A)	0.94	0.91
Amur (1)	8539.7(A)	8389.1(A)	8368.2(A)	0.94	0.92
Amur (2)	10146(A)	9574(A)	10208(A)	0.51	0.68
Li-Wu	3573.9(A)	3335.4(A)	2940.1(A)	0.37	0.40
Yufeng	1575.6(A)	1836.8(A)	1637.8(A)	0.45	0.35
Sandimen	3083.7(A)	3154.3(A)	3804.2(A)	0.43	0.48
Xinfadaqiao	6426(A)	6566(A)	8341(A)	0.19	0.34
			Monthly Maximum (m³/s)		
Tone	596.8(A)	592.0(A)	773.3(A)	0.12	0.14
Ishikari	1441.2(A)	1121.7(A)	1316.8(A)	0.09	0.06
Shinano	1079.3(A)	1129.6(A)	1241.3(A)	0.70	0.77
Yodo	659.8(A)	620.3(A)	802.1(A)	0.53	0.86
Chikugo	261.7(B)	343.4(AB)	488.7(A)	**0.0209**	**0.0108**
Changjiang	43626(A)	44528(A)	41996(A)	0.24	0.41
Songhuajiang	2959(A)	3282.9(A)	3229.5(A)	0.75	0.89
Yongding	124.0(A)	91.9(A)	82.1(A)	0.29	0.65
Jinghe	172.4(A)	194.1(A)	190.9(A)	0.84	0.74
Wujiang	3121.8(A)	3382.2(A)	2677.3(A)	0.11	0.09
Huanghe (Yellow River)	3438.6(A)	3758.5(A)	3286.0(A)	0.59	0.70
Beijiang	3645.6(A)	2946.1(A)	3145.6(A)	0.36	0.51
Dongjiang	1945.7(A)	1712.9(A)	1977.1(A)	0.65	0.68
Yana	3774.3(AB)	4454.3(A)	3609.2(B)	**0.0311**	**0.0320**
Pnezhina	4161.4(A)	3898.0(A)	4318.8(A)	0.79	0.66
Indigirka	5934.4(B)	6877.8(A)	5813.0(B)	**0.0209**	**0.0400**
Lena	75147(A)	73813(A)	72925(A)	0.84	0.68
Shilka	1279.9(A)	1304.0(A)	1237.6(A)	0.91	0.67
Kamchatka	1853.6(a)	1920.7(A)	1814.2(A)	0.55	0.60
Amur (1)	20283(A)	20950(A)	21167(A)	0.86	0.94
Amur (2)	22162(A)	22793(A)	24242(A)	0.54	0.58
Li-Wu	11105(A)	9342(A)	10195(A)	0.60	0.59
Yufeng	5297(A)	6157(A)	5794(A)	0.73	0.72
Sandimen	12663(A)	14627(A)	16919(A)	0.34	0.41
Xinfadaqiao	21937(A)	25725(A)	32962(A)	0.20	0.28

Table 4. Duncan Test, ANOVA, and Kruskall-Wallis (K.W.) Results for the Discrimination of El Niño, La Niña, and Neutral Years in the Far East Area (Continued)

River	*La Niña*	*Neutral*	*El Niño*	*ANOVA*	*K.W.*
	Mean	*Mean*	*Mean*	*P-value*	*P-value*
			Monthly Minimum (m³/s)		
Tone	96.0(A)	104.1(A)	95.2(A)	0.58	0.98
Ishikari	187.4(A)	181.9(A)	212.3(A)	0.34	0.41
Shinano	248.0(A)	247.8(A)	259.7(A)	0.90	1.00
Yodo	109.8(A)	108.9(A)	133.6(A)	0.27	0.24
Chikugo	36.2(B)	41.3(AB)	47.7(A)	0.08	0.13
Changjiang	7272.6(A)	6786.5(A)	6984.8(A)	0.33	0.28
Songhuajiang	205.4(A)	187.9(A)	214.0(A)	0.72	0.94
Yongding	9.6(B)	10.3(B)	14.7(A)	**0.0372**	0.14
Jinghe	16.5(A)	17.8(A)	16.8(A)	0.65	0.81
Wujiang	293.3(A)	279.8(A)	259.2(A)	0.51	0.54
Huanghe (Yellow River)	420.5(A)	405.4(A)	458.8(A)	0.68	0.66
Beijiang	300.1(A)	224.8(B)	200.3(B)	**0.0083**	**0.0394**
Dongjiang	295.6(A)	266.2(A)	310.3(A)	0.72	0.92
Yana	0.43(A)	0.10(A)	1.00(A)	0.16	0.36
Pnezhina	22.6(A)	20.9(A)	19.4(A)	0.59	0.58
Indigirka	7.63(A)	7.64(A)	7.94(A)	0.94	0.96
Lena	2107.4(A)	1351.9(A)	1459.8(A)	0.32	0.19
Shilka	3.42(A)	3.70(A)	3.71(A)	0.93	0.74
Kamchatka	393.5(A)	370.6(A)	387.5(A)	0.21	0.34
Amur (1)	605.3(A)	612.1(A)	617.3(A)	0.98	0.98
Amur (2)	1085.1(A)	1042.3(A)	1039.2(A)	0.95	0.77
Li-Wu	1218.0(A)	1036.5(A)	1006.5(A)	0.23	0.29
Yufeng	456.4(A)	444.6(A)	373.6(A)	0.47	0.43
Sandimen	58.3(A)	62.0(A)	73.6(A)	0.37	0.23
Xinfadaqiao	1338.5(A)	1016.9(A)	1123.9(A)	0.16	0.12

Numbers with a common letter between parenthesis are not discriminated by the Duncan test on the equality of several mean values. Bold and underline indicate a significant result at the 5 percent significance level.

ANOVA and Kruskall-Wallis tests are presented for the discharge data (mean yearly, monthly maximum, and monthly minimum) when tested for significant differences using the previously described statistical techniques. From these tables, one can see that for all three yearly discharge characteristics under consideration (mean, maximum and minimum monthly values), the Oceania Pacific area contains the most numerous rivers where El Niño/La Niña effects on discharge have been detected. The Far East, South East Asia, and the Indian Subcontinent present some teleconnection to the El Niño phenomenon, whereas Central Asia presents none.

Generally, when the El Niño years (warm events, with reference to the sea water temperature on the Southern Pacific Peruvian shore around Christmas; low SOI), tested significantly different from other years, they produced a low hydraulicity: less discharge than neutral, normal years, and can thus be qualified as dry. On the other hand, La Niña years (cold events; high SOI) generally produced a high hydraulicity: more discharge than neutral, normal years, and can thus be qualified as wet. These results concord with Simpson et al. (1993) even though these authors study the natural discharges (adjusted for water storage and release practices) rather than the actual measured discharges as for this paper. The agreement of the results with Simpson et al. (1993) indicates that human interventions on streamflow do not mask the relationships between the ENSO signal and streamflow, at least for the Oceania-Pacific region.

Table 5. Duncan Test, ANOVA, and Kruskall-Wallis (K.W.) Results for the Discrimination of El Niño, La Niña, and Neutral Years in the Indian Subcontinent Area

River	*La Niña*	*Neutral*	*El Niño*	*ANOVA*	*K.W.*
	Mean	*Mean*	*Mean*	*P-value*	*P-value*
		Mean Yearly Flows (m^3/s)			
Mahawell Ganga	69.7(A)	66.3(A)	60.2(A)	0.39	0.29
Gin Ganga	64.3(A)	61.8(A)	57.8(A)	0.30	0.19
Kamali	1420.5(A)	1380.3(A)	1273.6(A)	0.47	0.28
Kali Gandaki (1)	643.9(A)	570.6(AB)	439.9(B)	**0.0410**	0.10
Kali Gandaki (2)	49.51(A)	418.1(B)	392.0(B)	**0.0162**	**0.0478**
Tamur	533.5(A)	493.8(AB)	419.5(B)	**0.0268**	**0.0239**
Ganges (1)	11565(A)	11476(A)	10360(A)	0.33	0.18
Ganges (2)	14051(A)	12479(AB)	10835(B)	**0.0102**	**0.0189**
Sapt Kosi	1688.1(A)	1661.0(A)	1472.3(A)	0.14	0.09
Godavari	3028.5(A)	3186.1(A)	2828.1(A)	0.48	0.52
Krishna	1818.3(A)	1607.5(A)	1502.3(A)	0.17	0.49
Narmada	323.3(A)	296.4(A)	280.3(A)	0.87	0.34
		Monthly Maximum (m^3/s)			
Mahawell Ganga	171.1(A)	158.6(A)	149.2(A)	0.64	0.56
Gin Ganga	134.4(A)	135.4(A)	134.5(A)	0.99	0.96
Kamali	4336.9(A)	4445.3(A)	4052.3(A)	0.65	0.62
Kali Gandaki (1)	1646.7(A)	1434.0(A)	1354.8(A)	0.42	0.40
Kali Gandaki (2)	974.5(A)	832.7(B)	841.2(B)	**0.0341**	0.05
Tamur	1067.2(A)	990.2(A)	954.2(A)	0.40	0.35
Ganges (1)	39183(A)	41743(A)	39095(A)	0.59	0.85
Ganges (2)	50408(A)	45465(AB)	41615(B)	0.11	0.17
Sapt Kosi	5112.3(A)	4683.5(A)	4603.4(A)	0.47	0.43
Godavari	12428(A)	14018(A)	14201(A)	0.48	0.53
Krishna	7186.1(A)	6965.3(A)	6947.1(A)	0.94	0.97
Narmada	1727.0(A)	1541.4(A)	2094.2(A)	0.73	0.25
		Monthly Minimum (m^3/s)			
Mahawell Ganga	15.8(A)	14.5(A)	11.1(A)	0.48	0.26
Gin Ganga	20.1(A)	20.1(A)	15.5(A)	0.13	0.19
Kamali	323.4(A)	307.4(A)	324.2(A)	0.76	0.51
Kali Gandaki (1)	99.7(A)	104.6(A)	97.5(A)	0.82	0.84
Kali Gandaki (2)	99.9(A)	83.4(A)	105.2(A)	0.32	0.39
Tamur	92.8(A)	105.8(A)	86.5(A)	0.66	0.80
Ganges (1)	1893.6(A)	1668.7(A)	1666.8(A)	0.38	0.21
Ganges (2)	1804.0(A)	1719.6(A)	1675.3(A)	0.67	0.81
Sapt Kosi	328.2(A)	352.3(A)	341.3(A)	0.25	0.28
Godavari	59.8(A)	81.7(A)	64.4(A)	0.27	0.18
Krishna	18.3(A)	23.3(A)	19.0(A)	0.84	**0.0229**
Narmada	2.22(A)	1.82(A)	1.50(A)	0.55	0.67

Numbers with a common letter between parenthesis are not discriminated by the Duncan test on the equality of several mean values. Bold and underline indicate a significant result of the 5 percent significance level.

To this general situation, New Zealand presents an interesting and remarkable exception. The Mataura River exhibits higher discharge during El Niño years than during neutral years, which are also themselves higher than La Niña years – a situation opposite to the one prevailing for most affected rivers within the areas under study. This makes the New Zealand situation a special case. The Motu river located in the northeast region of the archipelago exhibits a significant dry El Niño signal, the Mataura river in the southwest of the archipelago shows a significant wet El Niño signal, and the three rivers in between (the Ongarue, Hurunui, and Ahuriri) show no teleconnection at all. This needs to be confirmed through analysis on a finer monthly scale, but it is probably the result of some orographic effects and of differentiated local wind directions. Moss et al. (1994) show a pattern for the Clutha river similar to the one of the Mataura river. The Clutha river is also in South New Zealand, so this result supports the opposite effect of the ENSO signal in south versus north New Zealand.

In its Climate Impacts Database, the Greenpeace Organization states: "The effects of El Niño are being felt in New Zealand. In normal seasons between El Niño events, easterly and northeasterly winds predominate, bringing rain to the north and east of the country, and drier conditions to the west and south. During El Niño events such as the current protracted one, drought is common in the north and east of the country, while the south and west are likely to experience heavy summer rain. Until the Southern Oscillation returns to the La Niña state, this situation is likely to continue. (Go south to duck El Niño dry period, New Zealand Farmer, 28 September 1994). One way to look at it is that the dry weather touring in the North Island would balance the wet weather in the south of the South Island. The South Island west coast is always wet anyway..."

Figure 2 maps the geographical distribution of the stations teleconnected to the phenomenon and shows which ENSO phase relates to this signal. The figure shows that most rivers in Australia, the Indian subcontinent, and, surprisingly, some rivers of northeastern Siberia seem to be affected mainly by the La Niña phase of the ENSO phenomenon, whereas rivers in Eastern Australia, Japan, Taiwan, and Central China seem more responsive to the El Niño phase. New Zealand exhibits a very mixed response, probably as the result of local orographic effects. A line joining southern Japan to the Caucasus could thus be seen as the northern limit of the ENSO influence.

Composite Analysis

The composite analysis allows a more detailed description of the temporal ENSO influence on river discharge. Since the Oceania-Pacific region is the most highly influenced region, a more complete composite analysis was performed on this region and the results were compared to summary results for the other regions.

First, streamflow indices were constructed for all 19 rivers in the Oceania-Pacific region to compare the patterns from river to river. (These individual streamflow indices are not presented in this paper.) The composite analyses on individual river streamflow indices show that the temporal patterns of the relationships are very similar for the majority of rivers in the Oceania-Pacific region but

Table 6. Duncan Test, ANOVA, and Kruskall-Wallis (K.W.) Results for the Discrimination of El Niño, La Niña, and Neutral Years in the South East Asia Area

River	*La Niña*	*Neutral*	*El Niño*	*ANOVA*	*K.W.*
	Mean	*Mean*	*Mean*	*P-value*	*P-value*
		Mean Yearly Flows (m^3/s)			
Pampanga	215.6(A)	224.7(A)	251.5(A)	0.56	0.75
Bonga	21.4(A)	28.5(A)	25.6(A)	0.38	0.27
Kelantan	629.7(A)	507.0(A)	566.1(A)	**<u>0.0447</u>**	**<u>0.0384</u>**
Mekong (1)	8065.1(A)	8043.0(A)	7557.5(A)	0.32	0.37
Nam Chi	239.2(A)	256.5(A)	228.9(A)	0.66	0.89
Nam Mun	556.9(A)	666.2(A)	620.0(A)	0.40	0.57
Nan	192.0(A)	186.8(A)	138.0(B)	**<u>0.0395</u>**	**<u>0.0375</u>**
Mekong (2)	2761.4(A)	2681.0(A)	2722.5(A)	0.90	0.85
Mekong (3)	7413.6(A)	7096.7(A)	6671.8(A)	0.40	0.35
		Monthly Maximum (m^3/s)			
Pampanga	707.6(A)	730.2(A)	854.6(A)	0.52	0.92
Bonga	83.6(A)	109.6(A)	110.2(A)	0.38	0.35
Kelantan	1669.3(A)	1230.6(A)	1584.7(A)	0.21	0.42
Mekong (1)	23383(A)	23778(A)	22099(A)	0.38	0.33
Nam Chi	796.8(A)	826.2(A)	860.1(A)	0.88	0.77
Nam Mun	2018.5(A)	25443.1(A)	2514.9(A)	0.32	0.21
Nan	728.6(A)	752.9(A)	545.3(A)	0.20	0.14
Mekong (2)	7350.1(A)	6801.2(A)	6723.4(A)	0.69	0.54
Mekong (3)	21311(A)	20254(A)	18988(A)	0.54	0.62
		Monthly Minimum (m^3/s)			
Pampanga	25.2(A)	22.6(A)	24.9(A)	0.85	0.98
Bonga	1.30(A)	1.85(A)	1.50(A)	0.52	0.66
Kelantan	304.4(A)	228.0(A)	225.2(A)	0.11	0.05
Mekong (1)	1549.8(A)	1410.7(A)	1491.8(A)	0.09	0.18
Nam Chi	23.0(A)	30.8(A)	27.6(A)	0.66	0.66
Nam Mun	44.3(A)	55.4(A)	51.3(A)	0.69	0.66
Nan	20.9(A)	23.7(A)	20.1(A)	0.61	0.92
Mekong (2)	807.9(A)	809.7(A)	839.1(A)	0.65	0.74
Mekong (3)	1381.8(A)	1391.5(A)	1562.9(A)	0.18	0.38

Numbers with a common letter between parenthesis are not discriminated by the Duncan test on the equality of several mean values. Bold and underline indicate a significant result of the 5 percent significance level.

Table 7. Duncan Test, ANOVA, and Kruskall-Wallis (K.W.) Results for the Discrimination of El Niño, La Niña, and Neutral Years in the Central Asia Area

River	*La Niña*	*Neutral*	*El Niño*	*ANOVA*	*K.W.*
	Mean	*Mean*	*Mean*	*P-value*	*P-value*
		Mean Yearly Flows (m^3/s)			
Amu-Darya	1261.1(A)	1494.4(A)	1240.7(A)	0.08	0.13
Zaravchan	156.4(A)	154.1(A)	154.8(A)	0.94	0.96
Gunt	101.6(A)	107.1(A)	100.1(A)	0.51	0.53
Vakhsh	631.8(A)	652.4(A)	622.4(A)	0.64	0.78
Biya	465.4(A)	474.6(A)	500.0(A)	0.47	0.36
Ob	12776(A)	12414(A)	12527(A)	0.83	0.72
Tom (1)	659.3(A)	630.1(A)	685.0(A)	0.19	0.30
Tom (2)	1057.7(A)	1008.9(A)	1101.7(A)	0.55	0.73
Tura	181.7(A)	186.6(A)	205.6(A)	0.72	0.98
Yenisei	17821(A)	18255(A)	17940(A)	0.59	0.45
Syr-Darya	500.9(A)	595.2(A)	460.9(A)	0.21	0.21
Urai	280.3(A)	278.8(A)	362.6(A)	0.36	0.37
Naryn	363.2(A)	375.5(A)	344.7(A)	0.61	0.72
		Monthly Maximum (m^3/s)			
Amu-Darya	2962.5(A)	3514.1(A)	3110.0(A)	0.28	0.37
Zaravchan	473.9(A)	474.3(A)	445.8(A)	0.50	0.62
Gunt	325.2(A)	355.6(A)	355.4(A)	0.63	0.53
Vakhsh	1648.9(A)	1715.0(A)	1590.0(A)	0.57	0.53
Biya	1400.8(A)	1399.8(A)	1417.7(A)	0.99	0.89
Ob	34177(A)	32973(A)	33629(A)	0.57	0.59
Tom (1)	3124.6(A)	2817.4(A)	3003.6(A)	0.27	0.08
Tom (2)	4219.7(A)	4602.3(A)	5060.6(A)	0.45	0.48
Tura	755.2(A)	777.0(A)	1093.6(A)	0.24	0.71
Yenisei	76500(A)	77989(A)	79740(A)	0.76	0.80
Syr-Darya	954.9(A)	1154.7(A)	945.4(A)	0.29	0.31
Urai	1504.6(A)	1461.9(A)	1746.6(A)	0.77	0.49
Naryn	921.8(A)	922.7(A)	893.6(A)	0.96	0.81
		Monthly Mimimum (m^3/s)			
Amu-Darya	313.8(A)	431.9(A)	318.7(A)	0.19	0.15
Zaravchan	34.8(A)	34.3(A)	36.4(A)	0.39	0.73
Gunt	26.0(A)	26.1(A)	25.0(A)	0.23	0.27
Vakhsh	180.8(A)	170.0(A)	172.9(A)	0.29	0.29
Biya	58.3(A)	52.6(A)	52.9(A)	0.15	0.27
Ob	3303.6(A)	3186.4(A)	3315.4(A)	0.74	0.92
Tom (1)	68.7(A)	67.6(A)	71.4(A)	0.78	0.78
Tom (2)	124.6(A)	125.9(A)	138.0(A)	0.71	0.78
Tura	25.0(A)	24.2(A)	23.1(A)	0.78	0.89
Yenisei	5133.3(A)	4914.3(A)	5437.5(A)	0.55	0.44
Syr-Darya	2451.(AB)	292.6(A)	187.1(B)	0.09	0.10
Urai	45.6(A)	44.7(A)	52.1(A)	0.59	0.48
Naryn	146.1(A)	134.7(A)	126.2(A)	0.47	0.42

Numbers with a common letter between parenthesis are not discriminated by the Duncan test on the equality of several mean values. Bold and underline indicate a significant result of the 5 percent significance level.

that their amplitudes differ. On the other hand, the Mataura river shows reversed Niño-Niña effects.

Figure 3 presents two 36-month Oceania-Pacific composite streamflow indices for El Niño (A), La Niña (B), and normal (C) years. The composite index formed with hatched bars is associated with all 19 rivers of the Oceania-Pacific region, while the solid bars consist of the composite index for rivers with a significant ENSO influence according to the ANOVA results (Mary[2], Darling, Mitchell, Avoca, Nymboida, and Motu). Note that the Mataura river was not used in the composite index of rivers with significant ENSO influence because the Niña-Niño effects for that river are opposite to the other rivers as indicated by the streamflow indices constructed for each river.

Figure 3A shows that for El Niño years, the streamflow index has negative mean values (zero represents the median) for a period of 18 months following the month of March of an El Niño year with a peak in the last five months of an El Niño year. The streamflow index shows that rivers in the Oceania-Pacific region tend to present low flows (lower than the median) for an 18-month period beginning in the month of April of an El Niño year and that one should expect particularly low flows in the last five months of an El Niño year.

Figure 3B shows that for La Niña years, the streamflow index has positive mean values for a period of

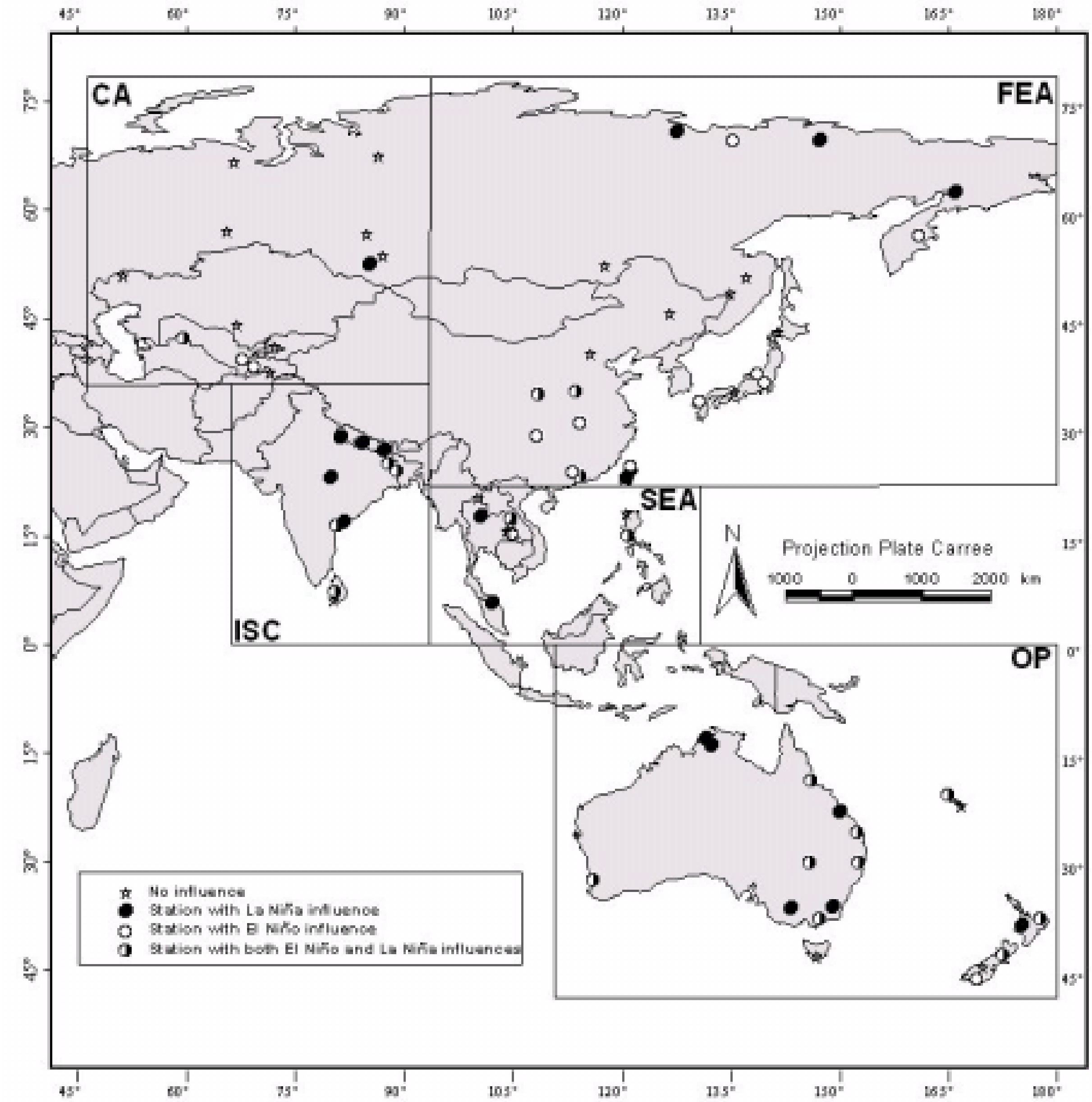

Figure 2. ENSO-River streamflow relationships for all the rivers studies. The size of the dots indicates the ENSO phases with a significant effect on river streamflow.

20 months following the month of March of a La Niña. However, the amplitude of the La Niña influence is smaller than the amplitude of the El Niño effect and the peak is not as precisely defined for the La Niña streamflow index. The streamflow index shows that the rivers of the Oceania-Pacific region tend to present high flows (larger than the median) for a 20-month period beginning in the month of April of a La Niña year but no month presents particularly high flows; however, one should expect higher flows during a La Niña year than during the following year.

Figure 3C shows no marked pattern, and small bars for normal years show that for years without El Niño or La Niña influences, the rivers tend to have streamflow on either side of the general median (meaning the median including all years: El Niño, La Niña, and Normal) producing a median for the normal years near the general median.

Figure 3 gives an indication of the regional pattern for rivers in the Oceania-Pacific region during El Niño or La Niña years. However, these patterns do not necessarily give a good indication of the effect for all rivers in the region. In order to assess rivers closely related to the regional composite streamflow index, Tables 8 and 9 present the mean square difference (MSD) and the mean bias between the Oceania-Pacific composite streamflow index and the streamflow index of each river. The mean bias for river k is:

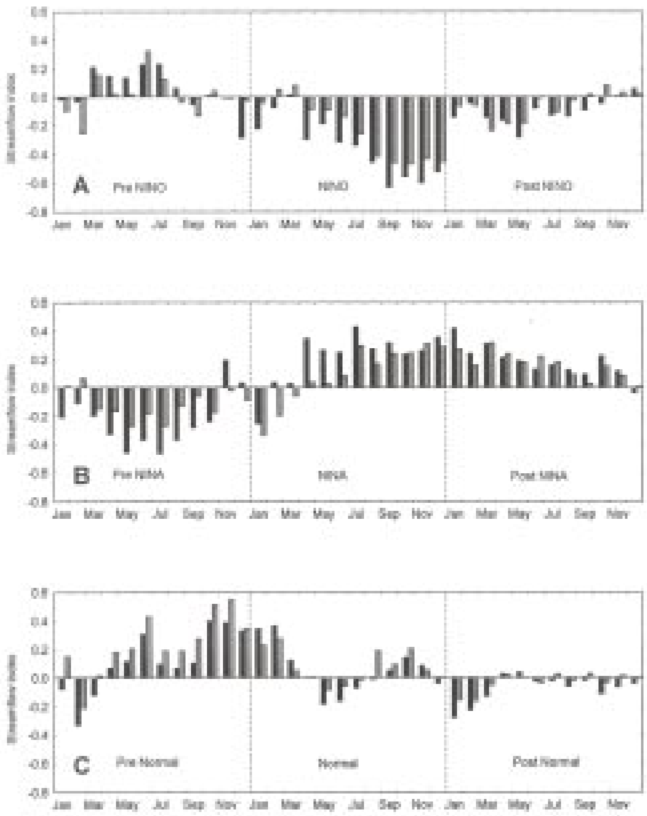

Figure 3. Regional composite streamflow indices in the Oceania-Pacific area. A = composite index for the years identified in an El Niño, phase, B = composite index for the years identified in a La Niña phase, and C = composite index for the years identified as normal. Solid bars are associated with rivers having a significant ENSO effect from analyses of variance and hatched bars are associated with all 19 rivers in teh Oceania-pacific area.

$$bias_k = \frac{\sum_{i=1}^{36}(s_{ki} - \bar{s}_i)}{36} \qquad (1)$$

where ski is the streamflow index for river k at month i (i=1, 36), and $\bar{s}_i$ is the regional composite streamflow index for month i (i=1, 36). The MSD for river k is:

$$MSD_k = \frac{\sum_{i=1}^{36}(s_{ki} - \bar{s}_i)^2}{36} \qquad (2)$$

The combined interpretation of these two statistics (mean bias and MSD) allows to distinguish between different levels of agreement between regional and individual streamflow indices. If both statistics are small, the regional streamflow index can be used to deduce the individual river streamflow relationship with the ENSO signal. If the MSD is large but corresponds approximately to the square of the mean bias, the pattern of the corresponding individual streamflow indices is similar to the pattern of the regional streamflow index, but a systematic bias for the months considered exists. If the MSD is large and the bias is small, the 36-month response of the individual river streamflow is different from the regional response to the ENSO signal.

Table 8 presents the years associated with an El Niño effect. For the 12 months of the El Niño, four rivers (Fitzroy, Mary[2], Nymboida, and Motu) show small MSD and biases indicating that the pattern of their streamflow indices are very similar to the pattern of the regional composite streamflow index. For these rivers, the regional El Niño effect can be used to characterize their streamflow in El Niño years. For post El Niño years, more rivers show patterns very similar to the pattern of the regional composite index. During El Niño years the Darling, Mitchell, and Avoca rivers are not completely explained by the regional composite index primarily because the El Niño effect in the regional composite index is not large enough (as indicated by the large negative bias and the MSD almost completely explained by the square of the bias). For these three rivers, we can expect an El Niño effect with a pattern similar to the regional composite index but with a greater amplitude than the one indicated by the regional index. For the other rivers, use of the regional composite streamflow index will tend to overestimate the effect of El Niño on streamflow of individual rivers and could even lead to erroneous conclusions, as in the case of the Mataura river.

Table 9 presents the possible use of the regional composite index to evaluate the streamflow patterns of individual rivers during La Niña years. Table 9 shows that few rivers present small MSD and bias values. The La Niña effect on the Avoca, Murrumbi, and Herbert Rivers could be deduced from the regional composite index, while the effect on the Mary[2], Mitchell, and Nymboida Rivers

Table 8. Comparison of the Streamflow Indices for Each River with the Oceania-Pacific Composite Streamflo Index for the El Niño Years

	Pre Niño Years		*Niño Years*		*Post Niño Years*	
	MSE	*Bias*	*MSE*	*Bias*	*MSE*	*Bias*
Fitzroy	0.12	0.27	0.03	-0.01	0.07	0.06
Mary2	0.03	0.10	0.01	-0.05	0.03	0.14
Darling River	0.21	0.37	0.10	-0.24	0.03	0.03
Mitchell River	0.12	0.25	0.10	-0.26	0.03	0.05
Avoca River	0.07	-0.02	0.10	-0.15	0.07	0.12
Nymboida	0.06	-0.14	0.04	-0.03	0.01	0.03
Motu	0.15	0.15	0.06	-0.04	0.07	-0.48
Daly	0.09	-0.15	0.08	0.24	0.02	-0.02
Herbert River	0.05	0.17	0.05	0.12	0.04	-0.02
Mary1	0.10	0.09	0.19	0.22	0.16	-0.24
Huon	0.12	0.17	0.22	0.31	0.05	0.01
Murrumbi	0.04	0.07	0.12	-0.31	0.02	0.05
Serpenti	0.27	0.07	0.16	0.13	0.21	0.12
Tipindje	0.43	0.41	0.15	-0.13	0.09	0.03
Riviere des lacs	0.34	-0.02	0.25	0.12	0.11	0.15
Ongarue	0.15	0.18	0.10	0.21	0.06	0.01
Hurunui	0.09	-0.08	0.27	0.29	0.10	0.19
Ahuriri	0.19	-0.28	0.12	0.14	0.10	0.19
Mataura	0.50	-0.63	0.58	0.70	0.05	0.17

Table 9. Comparison of the Streamflow Indices for Each River with the Oceania-Pacific Composite Streamflo Index for the La Niña Years

	Pre Niña Years		*Niña Years*		*Post Niña Years*	
	MSE	*Bias*	*MSE*	*Bias*	*MSE*	*Bias*
Fitzroy	0.82	-0.77	0.17	0.00	.06	0.16
Mary2	0.07	-0.05	0.08	0.20	0.03	-0.03
Darling River	0.16	-0.04	0.21	0.38	0.03	0.05
Mitchell River	0.09	0.19	0.06	0.16	0.05	-0.11
Avoca River	0.24	-0.29	0.09	-0.02	0.02	0.06
Nymboida	0.07	0.06	0.07	0.13	0.02	-0.59
Motu	0.16	-0.10	0.22	0.28	0.15	-0.21
Daly	0.21	0.31	1.24	-0.90	0.06	-0.04
Herbert River	0.06	-0.13	0.05	0.06	0.03	0.01
Mary1	0.44	-0.02	0.49	-0.36	0.15	0.09
Huon	0.18	0.22	0.11	-0.08	0.11	-0.26
Murrumbi	0.06	0.16	0.02	-0.01	0.04	-0.12
Serpenti	0.24	0.18	0.14	0.03	0.22	-0.26
Tipindje	0.30	0.33	0.29	-0.18	0.03	0.07
Riviere des lacs	0.47	0.36	0.27	-0.28	0.09	-0.09
Ongarue	0.59	-0.30	0.27	-0.09	0.05	-0.10
Hurunui	0.16	0.04	0.26	-0.12	0.13	-0.24
Ahuriri	0.31	0.20	0.24	-0.30	0.22	-0.40
Mataura	0.60	0.52	0.22	-0.33	0.18	-0.38

present a pattern similar to the regional index but are underestimated, as indicated by the positive bias.

While El Niño and La Niña effects were often detected in the ANOVA analyses for the Oceania-Pacific region, far less effects were detected in the other regions. Figure 4 presents the regional composite indices for Central Asia (Figure 4A), the Indian Subcontinent (Figure 4B), and South East Asia (Figure 4C). The figure shows that El Niño (solid bars) and La Niña (hatched bars) regional effects are not as well defined as in the Oceania-Pacific region. In Central Asia the regional effect appears to take place in the year following an El Niño (or La Niña) year and the effect would then be opposite in terms of hydraulicity (wet vs. dry) to that in the Oceania-Pacific region. In the Indian Subcontinent and South-East Asia there are no well-defined patterns. The absence of patterns in the regional streamflow index shows the absence of El Niño (or La Niña effects) or different effects from river to river resulting in no regional effect when the streamflow indices of individual rivers are averaged in a regional composite index.

From an operational point of view, the goal remains to be able to forecast the occurrence of abnormal high or low flows (floods/droughts) with a sufficient lead time in order to mitigate the extent of possible damage. The above results could be exploited as part of an agricultural or flood warning system, taking advantage of the fact that the development of the different phases of ENSO are actually forecasted several months in advance with reasonable accuracy by climatologists (by December, climatologists can determine if the following year will be Niño, Niña, or normal).

From a practical point of view, Tables 8 and 9 could be used to evaluate the streamflow patterns for expected monthly discharges during El Niño and La Niña events in several rivers of the Oceania-Pacific region. Because the effects are more significant in the latter months of the year, one could forecast several months in advance the appearance of abnormal flows, since an El Niño or La Niña year can be determined in the first months of the year. Other regions, according to the results presented in this paper, do not show as much possibility for forecasting the occurrence of abnormal flows.

Once the presence of an abnormal year is identified, the use of descriptive results from past observations allows the practical use of the results in this paper. For example, for the Darling River, which is highly influenced by the ENSO, past observations indicate that during the El Niño phase, the lowest monthly discharge occurs in September (158 m^3/s), whereas for the same month, the expected discharge is 2304 m^3/s and 1243 m^3/s for the La Niña and the neutral phases, respectively. Thus it may be prudent, in the case of an expected El Niño phase in the future, to store water in reservoirs or dams during the high flow period, in order to be able to release it later to main-

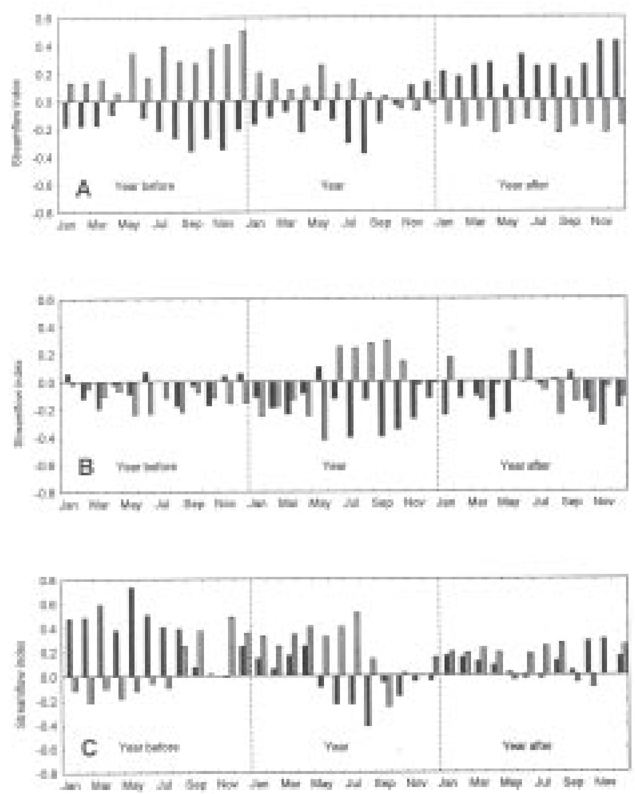

Figure 4. Regional composite streamflow indices in the Asia-Pacific area. A = regional composite index for the Central-Asia area, B = regional composite index for the Indian Subcontinent area, and C = regional composite index for South-East Asia. Solid bars are associated with years identified in an El Niño phase and hatched bars are associated with years identified in a La Niña phase.

tain a given river level for transportation or irrigation purposes or other urban or industrial uses.

Conversely, for the same river, high flows occur during the La Niña phase in August (8132 m^3/s) where, during the same month, only 876 m^3/s and 907 m^3/s are expected during El Niño and neutral phases, respectively. Given this situation, releasing some of the water stored in dams and reservoirs as soon as a La Niña phase is expected may be a good strategy to make room for the expected high flows and minimize the damage related to flooding. Even if the variability is quite large and some of the differences in discharge not quite statistically significant, the general direction of the mitigation strategies remains valid.

One should note that the values reported in this study are not related to the strength of the actual SOI index, but solely to the fact that they belong to a specific phase of the ENSO. As the forecasting power of the models relating the discharge to the SOI and other explaining factors improves, we will be able to refine and fine-tune mitigating strategies accordingly.

Conclusion

The database of world river discharge series maintained at the Global Runoff Data Centre (GRDC) was exploited to address the teleconnection between the ENSO phenomenon and recorded historical discharge of selected rivers in the Asia-Pacific region in order to assess the magnitude and timing of the impact on river discharges as well as the geographical extent of the influence of the ENSO-generated signal. It was found that its influence extends well beyond the South Pacific region and that all areas studied were more or less affected, with the notable exception of the most continental part of Asia.

The availability of a large discharge database means that global analyses can be performed, thus downplaying local unusual events whose explanation would have demanded detailed knowledge of the historical background of each river and water basin (knowledge that is currently lacking).

This study shows that in most areas of the Asia-Pacific region, an El-Niño-related signal can be detected in the historical river discharge series of some rivers stored at the Global Runoff Data Centre (GRDC). This signal is particularly strong in Australian rivers whose regimes are known to fluctuate widely. For most stations, this effect consists mainly of a reduction/amplification of the seasonal fluctuations for El Niño/La Niña-labelled events, respectively. In most instances in this part of the world, the El Niño phase of the ENSO is a relatively dry phase and the La Niña phase is a relatively wet phase compared to the unlabelled normal phases, but there are some exceptions.

The composite analysis identified the temporal patterns in the relationships between ENSO and river streamflow. A regional composite streamflow index in the Oceania-Pacific area indicates an overall regional pattern that can be generalized to several individual rivers. In other areas of the Asia-Pacific region, regionalization of the temporal pattern of the ENSO-streamflow relationship is less informative. Given the possibility of labelling a year as Niño or Niña as early as January and the patterns identified by the composite analysis (maximum effect in the last five months of a Niño or Niña year), the construction of a composite index appears to be a useful tool for forecasting wet and dry months or seasons related to ENSO phases.

Acknowledgements

The authors wish to express their gratitude to the collaborators of the Global Runoff Data Centre in Koblenz, Germany, for their warm reception and hospitality, and in particular to the director, Dr. W. Grabs, and Mr. M. Hils. Many thanks also to Mr. T. DeCouet who restructured the GRDC database to adapt its format to the statistical softwares used. Many thanks also to Dr. D. Kraemer and Dr. A. Askew of the Hydrology and Water Resources Department of the World Meteorological Organization in Geneva, Switzerland, for their encouragement and support.

About the Authors

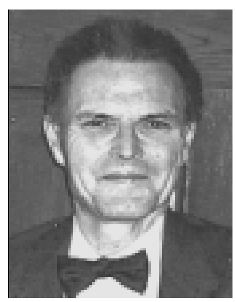

Daniel Cluis earned an engineering degree in hydraulics and a doctorate in fluid mechanics from the University of Grenoble (France). Since 1970, he took part of the development of the water research center of the University of Québec (INRS-Eau). His fields of interest include the mathematical modelization of contaminant transportation at the watershed scale and the adaptation of statistical methods to practical environmental problems. He can be reached at INRS-Eau, University of Québec, P.O. Box 7500, Sainte-Foy, Québec, Canada, G1V 4C7. Email: daniel_cluis@inrs-eau.uquebec.ca.

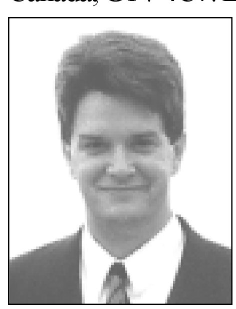

Claude Laberge earned a bachelor's degree in statistics and a master's degree in mathematics (statistics option) from Université Laval and completed his Ph. D. in water science at INRS-Eau (branch of the Université du Québec). He founded STATEX, a statistical consultant firm, in 1990. His domains of specialization are the application of statistics in environmental studies and in trend detection in time series. He can be reached at STATEX, 3332 de la Paix, Sainte-Foy, Québec, Canada, G1X 3W6. Email : claude.laberge@sympatico.ca.

Discussions open until December 1, 2002.

References

Chiew, F.H.S., T.C. Piechota, J.A. Dracup, and T.A. McMahon. 1998: "El Niño/Southern Oscillation and Australian Rainfall, Streamflow and Drought: Links and Potential for Forecasting." *J. Hydrol*. 204: 138–149.

Cluis, D. 1998. "Analysis of Long Runoff Series of Selected Rivers of the Asia-Pacific Region in Relation with Climate Change and El Ninõ Effects." *GRDC Report No.21*. Koblenz, Germany.

Conover, W.J. 1980: *Practical Nonparametric Statistics*. 2nd Ed. New York, New York, USA: John Wiley and Sons.

Dracup, J.A. and E. Kahya. 1994. "The Relationships Between U.S. Streamflow and La Niña Events." *Wat. Resour. Res*. 30, No. 7: 2133–2141.

Eltahir, E.A.B. 1996. "El Niño and the Natural Variability in the Flow of the Nile River." *Wat. Resour. Res.* 32, No. 1: 131–137.

Guetter, A.K. and K.P. Georgakakos. 1996. "Are the El Niño and La Niña Predictors of the Iowa River Seasonal Flow?" *Journ. Appl. Meteorology* 35: 690–705.

Hastenrath et al. (1993). "Diagnostic and Prediction of Anomalous River Discharge in Northern South America." *Journal of Climate* 3: 1080–1096.

Kahya, E. and J.A. Dracup. 1993. "U.S. Streamflow Patterns in Relation to the El Niño/Southern Oscillation." *Wat. Resour. Res*. 29, No. 8: 2491–2503.

Kim, Y.O. and H.S. Lee. 2000. "Korean Streamflow Patterns in Relation to El Niño/Southern Oscillation." *Water Engineering Research* 1, No. 2: 107–117.

Montgomery, D.C. 1984. *Design and Analysis of Experiments*. 2nd Ed. New York, New York, USA: John Wiley and Sons.

Moss, M.E., C.P. Pearson, and A.I. McKerchar. 1994. "The Southern Oscillation Index as a Predictor of the Probability of Low Streamflows in New Zealand." *Wat. Resour. Res.* 30, No. 10: 2717–2723.

NRC, 1996. *Learning to Predict Climate Variations Associated with El Niño and the Southern Oscillation*. Washington, DC, USA: National Reserch Council, Nat. Acad. Press.

Piechota, T.C., J.A. Dracup, and R.G. Fovell. 1997. "Western U.S. Streamflow and Atmospheric Circulation Patterns During El Niño Southern Oscillation (ENSO)." *J. Hydrol.* 201, Nos. 1-4: 249–271.

Piechota, T.C. and J.A. Dracup. 1996. "Drought and Regional Hydrologic Variation in the United States: Associations with the El Niño-Southern Oscillation." *Wat. Resour. Res*. 32, No. 5: 1359–1373.

Ropelewski, C. F. and P.D. Jones. 1987. "An Extension of the Tahiti-Darwin Southern Oscillation Index." *Mon. Weath. Rev*. 115: 2161–2165.

Ropelewski, C.F., M.S. Halpert, and V.E. Kouski. 1995. "Southern Oscillation-precipitation Relationships: Opportunities for Improved Predictions." In *Proc. Inter. Sci. Conf. On TOGA*. Melbourne 2-7 Apr. WCRP-91-WMO/TD Rep. No 717: 865–869.

Shukla, J. and D.A. Paolino. 1983. "The Southern Oscillation and Long Range Forecasting of the Summer Monsoon Rainfall over India." *Mon. Weath. Rev*. 111: 1830–1837.

Simpson, H.J., M.A. Cane, A.L. Herczeg, S.E. Zebiak, and J.H. Simpson. 1993. "Annual River Discharge in Southern Australia Related to El Niño Southern Oscillation Forecasts of Sea Surface Temperature." *Water. Resour. Res.* 29, NO. 11: 3671–3680.

Troup, A.J. 1965. "The Southern Oscillation." Quart. *J. Roy. Meteor. Soc*., 91, No. 390: 490–506.